ISBN: 978-3-95450-250-9 ISSN: 2673-5520 doi:10.18429/JACoW-MEDSI2023-THOBM02

FIRST RESULTS OF A NEW HYDROSTATIC LEVELING SYSTEM ON TEST PROCEDURES AT SIRIUS

W. R. Heinrich†, G.R.S. Gama, G.J. Montagner, E. Teixeira, S.P. Oliveira
Setup Automação, Campinas, Brazil
R. B. Cardoso, L. R. Leão, S. R. Marques, R. T. Neuenschwander
LNLS/CNPEM, Campinas, Brazil

Abstract

The Hydrostatic Leveling System (HLS) is commonly employed in Structural Health Monitoring (SHM) to anticipate issues in large-scale structures. Particularly in structures like particle accelerators, it is used in high-precision alignment, where small differences in elevation such as terrestrial tides, could affect machine operation. This study outlines the development and evaluation of the first HLS based in Linear Variable Differential Transformer (LVDT) and were used to monitor the structure at LNLS/CNPEM, Brazil, from 2020 to 2023. A comparative analysis with a capacitance-based off-the-shelf HLS was executed, and experimental data analyzed through Fast Fourier Transform (FFT) confirmed the presence of tidal components in both HLS's data. Additionally, the correlation between level and temperature data was demonstrated by Pearson coefficient. The Setup-HLS device, developed with support from Brazilian national resources, exhibited accurate measurements in building tilt and diurnal and semi-diurnal Earth tide variations. Future researches include a calibration jig and an online verification system. This research provides a viable alternative to existing HLS systems.

INTRODUCTION

The Hydrostatic Leveling System (HLS) is a precision measurement and monitoring system designed to detect differences in elevation between points in the system, typically achieving submicrometric precision and repeatability on the order of microns. This is accomplished by measuring the fluid's height difference, usually water, contained in a recipient, and the inclination between two points in the system where two sensors are located. Various technique principles are employed in HLS systems, including fiber optic and interferometric methods [1], ultrasonic technologies [2], capacitance and dielectric measurements [3], as well as mechanical and optical approaches [4].

The system is applied in diverse fields such as monitoring sea levels, water reservoirs, groundwater, dams, seismic events, building foundations, tunnels, traffic of heavy vehicles, and alignment of particle beams in accelerators. Generally, HLS is widely used in Structural Health Monitoring (SHM) to predict potential structural issues in large-scale equipment and facilities.

During the development of this system, it is crucial to meticulously isolate specific phenomena and sources of uncertainty that may influence measurement results, including tidal forces. Tidal forces result from spatial gradients in the gravitational field strength originating from celestial bodies. This gravitational phenomenon induces the elongation of the body experiencing the tidal force along the axis aligned with the center of mass of the attracted body.

The consequences of tidal forces encompass various occurrences on Earth, such as ocean tides, earth's rotation, tidal heating, tidal locking and terrestrial tides (or solid-earth tides). Careful consideration of tidal forces is essential for accurate and reliable HLS measurements.

On Earth, the principal manifestation of this gravitational interaction arises from the Moon's and Sun's gravitational influences, leading to the periodic oscillation of the semidiurnal of terrestrial tide, with a typical amplitude of approximately 0.55 meters [5]. Moreover, terrestrial tides and localized gravitational field variations contribute to minute perturbations in particle accelerator systems, on the order of 1 millimeter, as evidenced by measurements conducted in Geneva at the Large Electron-Positron Collider (LEP). The standard model of electroweak interactions requires precise knowledge of the LEP beam energy with an accuracy of 20 ppm. However, small fluctuations, induced by tidal effects, resulted in a beam energy variation of approximately 120 ppm [6].

HLS has been employed to precisely measure the tidal effect, which has well known periods and frequency components, so detecting these frequencies in the results measured by the HLS is a step in the sensor validation.

This study introduces a novel and robust HLS, denoted as Setup-HLS, which represents a pioneering application of the Linear Variable Differential Transformer (LVDT). The device is capable to quantify terrestrial tidal influences on level variations at the micrometer scale and was used for testing and structural monitoring at the Laboratório Nacional de Luz Síncrotron (LNLS-CNPEM) in Campinas, São Paulo, Brazil, from the years 2020 to 2023 [7, 8].

DEVICE CONCEPT

The Setup-HLS system employed in this study is an innovative Brazilian HLS, funded by FAPESP/FINEP. It was specifically designed for implementation at the Sirius facility and achieved a Technology Readiness Level of 9 (TRL 9) during its development, indicating proven functionality in an operational environment [9]. The configuration of the Setup-HLS comprises a cylindrical enclosure made of anodized aluminum, housing instrumentation responsible for converting analog water level signals into digital format. The analog signal originates from the core of the device, constructed from super permalloy and operated through a Linear Variable Differential Transformer (LVDT) system. The principal element in the core system configuration, including the LVDT, is shown in Fig. 1. The selection of materials and sensor configuration was motivated by their superior stability in the presence of high-frequency interference, resistance to temperature fluctuations, and cost-effectiveness compared to other alternatives.

The choice of acrylic as a material for the sensor housing and the use of LVDT as the working principle were aimed at mitigating the effect of temperature on sensor readings, in line with literature on HLS sensor design [10]. The shelter infrastructure includes a thermosensitive probe and a vibration transducer to accommodate the measuring rod's response to environmental conditions over an extended duration. The temperature transducer monitors laboratory temperature and assesses its influence on water level measurements. At the lower end of the apparatus, an opening is designated for water inflow, while an additional orifice is positioned at the upper end to facilitate the establishment of air pressure equilibrium.

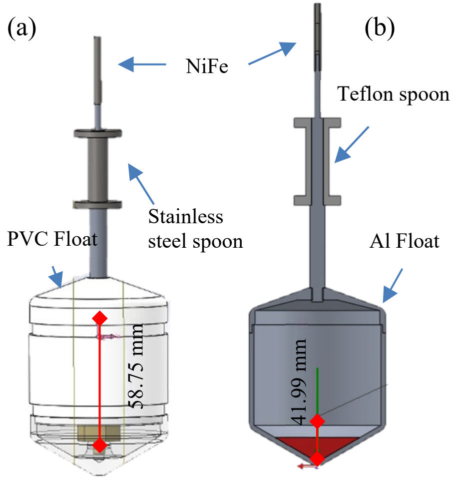

Figure 1: Float modification from (a) TRL5 to (b) TRL9.

As demonstrated in the next section, the tidal effect can be accurately measured when the friction between the steel spool and the housing does not impede the float's movement. Although the application of lubricant improved the situation, the gradual desiccation of the lubricant led to the cessation of the float's movement. To overcome this challenge, a PTFE spool was adopted as a replacement for the steel spool, as depicted in Fig. 1(b). Additionally, the vibration profile was altered to trigger more frequent movements, aiming to prevent friction-related issues.

Furthermore, an aluminum float was utilized to increase weight and lower the center of gravity, resulting in a more stable apparatus configuration. An analytical study was conducted to elevate the buoyancy center.

The device is equipped with a semiconductor electronic tilting system on the top of the cylinder, offering a resolution of 0.1° inclination. LED indicators, calibrated by three springs that hold the entire device body, facilitate the tilting system. The springs are connected to a stainless-steel ring that can be fixed in any location using screws.

These LEDs were employed for coarse calibration during the installation and commissioning of the beamlines at Sirius. A LabView software was developed and utilized for fine slope calibration, as well as for hydrostatic level and temperature measurements (in the laboratory) as a preliminary test.

Electronic communication is facilitated by a self-made circuit requiring a 24V power supply and utilizing RS-232 to transmit LVDT AD converted displacement and temperature data to the acquisition software. Three images of the Setup-HLS are provided in Fig. 2: (a) Setup-HLS without case protection, (b) PTFE spool and permalloy core, and (c) on-site. A subjective comparative analysis with other types of HLS is presented in Table 1.

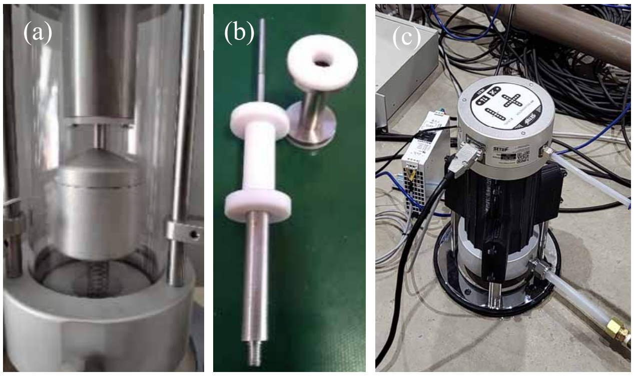

Figure 2: (a) Aluminum float, (b) PTFE spoon (c) Setup-HLS on the top Sirius ring accelerator's shell.

Table 1: Feature Comparison of Different Types of HLS

Features	**Technique Principles***		
	F.O.I.	**U.T.**	**C.D.**
Resolution (S.N.)	10^{-12}m	10^{-5}m	10^{-6}m
Fluid dependence	No	Yes	Yes
Temperature influence	Free	+	++
Magnetic field influence	Free	Free	+
Eletric field influence	Free	+	+
Air humidity influence	Free	Free	+
Price (x EUR1000/point)	>160.0	>20.0	>8.0

*S.N.: Scientific Notation, F.O.I.: Fiber Optic and Interferometric, U.T.: Ultrasonic Technologies and C.D.: Capacitance and Dielectric.

It is observed that HLS Fiber Optic and Interferometric exhibits the highest resolution, no influences from other external variables, but comes at a higher cost. On the other hand, HLS Capacitance and Dielectric offers good resolution, compared to HLS Ultrasonic Technologies, but at a lower cost.

The Setup-HLS features resolution in the micrometer range. Additionally, the acrylic transparent coating allows for visual inspection and integration with computer vision using a microscopic lens for measurement validation. Moreover, the material exhibits a thermal expansion coefficient close to that of water (both ~68.0 µm/m-°C at 20.0 °C), nullifying the effect of temperature-induced container shape modification, despite this, the new HLS does not depend on the type of fluid thus enabling the use of synthetic fluid that may have some advantage due to functional physicochemical characteristics. Their calibration relies solely on the interchangeability of the upper ogive of the devices, without affecting the operation of the HLS network. The device has a lower susceptibility to electric and magnetic fields compared to the Capacitance and Dielectric and no humidity influence. The temperature influence will be analyzed in the following section.

EXPERIMENTAL PROCEDURE

The Setup-HLS was securely anchored to the top of the concrete shielding of the accelerator at four evenly spaced points, each 90° apart around the circumference of the accelerator. To investigate the effects of tidal phenomena, a pre-installed pipeline developed by Sirius, containing a heterogeneous solution of water and air, was utilized. This pipeline was connected to a capacitance-based off-the-shelf HLS, which had previously been used to measure tidal effects. At Sirius, the capacitance-based HLS configuration comprises 20 devices operating continuously [11]. The Setup-HLS arrangement was meticulously linked to the capacitance-based HLS via the pipeline at four points.

Water levels were continuously measured by the Setup-HLS over three years, but for the purposes of this study, data from a one-week period were analyzed, encompassing measurements of both temperature and pipeline hydrostatic variation. The Setup-HLS recorded temperature and water variation every 756 seconds, while the capacitance-based HLS was configured to collect data at a more frequent interval of 31 seconds. The acquisition time was determined by the Sirius team managing the experiment. The resulting data has been collected and will be presented in the forthcoming section.

RESULTS AND DISCUSSION

In this section, we present the Setup-HLS dataset for the evaluation of hydrostatic leveling fluctuations and a comprehensive statistical analysis of the gathered data was executed, establishing correlations between the outcomes obtained from a commercially available capacitance-based HLS deployed concurrently at the same measurement site.

The Sirius accelerator facility is structured with 60 distinct circular structural axes, and the Setup-HLS sensor is positioned along four specific axes designated as 14, 29, 44, and 59. It is worth noting that the HLS on axis 59 encountered a mechanical locking issue, and the results obtained from this axis were excluded from the analysis.

The data depicted in Fig. 3 correspond to axes 14 and 29. Graph (a) illustrates a noticeable decreasing tendency in water level at the first axis, while graph (b) shows an increasing tendency in the level on the second axis, which is spaced 15 axes apart. This dataset, pertaining to level measurements, may indicate a building tilt.

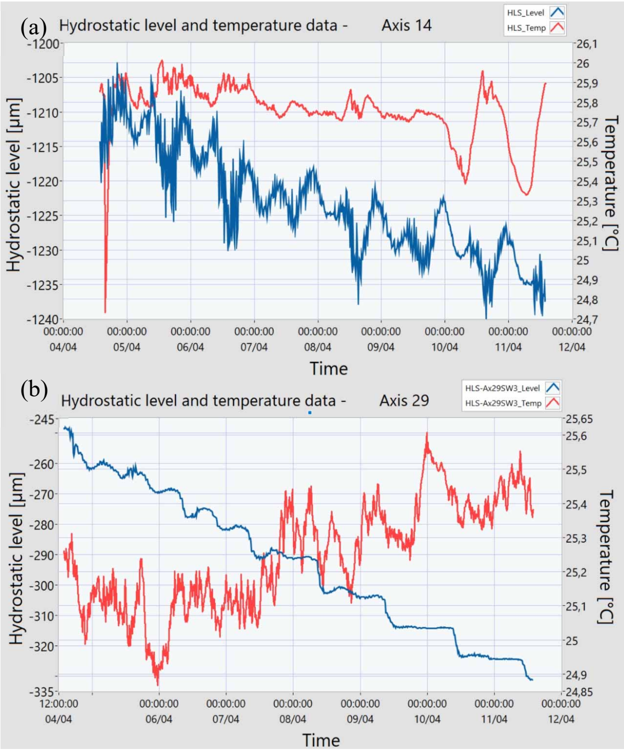

Figure 3: Graph presenting hydrostatic level (blue) and temperature measurements (red) for the period, from Setup-HLS (a) Axis 14, (b) Axis 29.

Based on these initial observations, software has been developed using LabVIEW to process measurement data for both sensors, Setup-HLS, and capacitance-based HLS. The software provides metrics to assess device performance linked to two goals: 1) The ability to detect real physical phenomena through hydrostatic level measurement; 2) Studying the interdependence between level measurement and temperature data.

A brief description of the calculations performed will be provided: For goal 1, a conspicuous oscillatory pattern with an estimated periodicity of approximately 12 hours can be observed in Fig. 3, representing the tidal effect. A Fast Fourier Transform (FFT) analysis was conducted on level measurement data for both devices installed on axis 14. This analysis allowed the identification of components of the terrestrial tide frequency. The absolute values of the four main FFT components and their frequencies were listed and can be seen in Table 1.

Components with frequencies corresponding to periods larger than 33.68 hours were ignored. As presented in [12], a model for Earth tides in the state of Sao Paulo is proposed, based on gravitometer measurements. The main diurnal and semidiurnal components identified are M2, S2, and K1, corresponding to tidal periods of 12h25m, 12h, and 23h56m, respectively [13]. As seen in Table 2, these main components are present in the results of the FFT analysis for both sensors, among the four most significant components found. It can be inferred from the frequency values for the components listed. It is noted that for Setup-HLS, the 23h56m component is slightly more significant than the 12h component.

Table 2: Main FFT Components for Level Measurement

Setup-HLS FFT components		**Capacitance-based HLS FFT components**	
Period (hours)	**Intensity** (mm)	**Period** (hours)	**Intensity** (mm)
24.06	24.68	24.00	17.39
12.03	22.50	12.00	26.06
16.84	13.10	12.92	10.96
12.96	12.96	11.20	7.20

For goal 2, level and temperature data were individually considered for each sensor, whether Setup-HLS or the capacitance-based HLS. Both level and temperature data were scaled to the [-1, +1] range and filtered using a 3rd-order Butterworth high-pass filter with a cutoff frequency equivalent to a 6.944-hour period. Pearson coefficient calculations were performed between the values in resulting data, and the results are listed in Table 3 for both Setup and capacitance-based sensors.

Table 3: Pearson Coefficient between Hydrostatic Level Measurement and Temperature Data for Both Sensors with 31-Second Interval

Location on Sirius	**Level to Temperature – Pearson Coefficient**	
	Setup-HLS	**Capacitance-based HLS**
Axis 14	0.42	0.43
Axis 29	0.37	0.84
Axis 44	0.61	0.91
Axis 59	0.03	0.45

As observed, higher absolute values for Pearson correlation between water level and temperature signals were noted in capacitance-based sensors compared to HLS Setup sensors, for both measured periods. As shown in [14] a simulation was developed in the same laboratory investigating the amplitude of thermal displacement on the concrete ring shield. These results point to displacement of up to 80 microns in radial direction at 1.5 degrees Celsius of temperature variation. Although the work did not provide enough information to estimate the final contribution to the vertical uncertainty displacement estimation, it demonstrates the need to evaluate HLS sensors in a calibration process that properly isolate the uncertainties components.

CONCLUSIONS

The Setup-HLS was able to accurately measure the effects of tides and building tilt over time, and probably will detect several geological factors with similar amplitude such as changes in the water table, seismic oscillations, earth quakes, etc. After 30 months of level/tilt monitoring it became apparent that there were challenges in isolating uncertainty components and system interferences to HLS measurements. These challenges included influences such as ambient temperature in the measurements, changes in the physical state and treatment of water within the container or even biological effects as the observed growth of algae in the hydrostatic channels. In this paper the strategy of isolating a known terrestrial tide periodic effects to compare the measurements between HLSs were successfully demonstrated. The complexity for isolating each uncertainties components at the submicron order of magnitude at the field, indicates that is recommended to periodically perform system calibration and reliability analysis for measurement repeatability, to verify sensor manufacture's declared specifications and proper system operation.

For future works, a calibration jig is currently been proposed in order to allow statistical analysis of measurement uncertainties and also to study the behavior of the HLS sensors; there is also a possibility for simple system verification using an online testing aiming to map unknown interferences over the time. In addition, interference of the electromagnetic field and concrete expansion influences to device measurements are a relevant field of study.

REFERENCES

[1] A. Herty *et al.*, "Hydrostatic Levelling Sensors Based on Extrinsic Fibre Fabry-Perot Interferometer Technology", in *Proc. 14th International Workshop on Accelerator Alignment*, Grenoble, France, Oct. 2016.

[2] H. J. Choi *et al.*, "Operation Status of HLS System Installed to Measure Ground Change of Large Scientific Equipment in Real Time", in *Proc. MEDSI'18*, Paris, France, Jun. 2018, pp. 245-248. `doi:10.18429/JACoW-MEDSI2018-WEPH18`

[3] T. Morishita and M. Ikegami. "The slow-ground-motion monitoring based on the hydrostatic leveling system in J-PARC linac", *Nucl. Instrum. Methods Phys. Res., Sect. A*, vol. 602, pp. 364-371, Apr. 2009. `doi: 10.1016/j.nima.2009.01.152`

[4] S. F. Xu, X. Y. He, P. Wang, W. Wang, and Q. Y. Yao, "Analysis of Tidal Effects on Measurement Accuracy of HLS", in *Proc. IPAC'13*, Shanghai, China, May 2013, paper WEPME027, pp. 2989-2991.

[5] G. Petit and B. Luzum, IERS Conventions (2010), `http://www.iers.org/TN36/`

[6] L. Arnaudon *et al.*, "Effects of terrestrial tides on the LEP beam energy", *Nucl. Instrum. Methods Phys. Res., Sect. A*, vol. 357, pp. 249-252, Apr. 1995. `doi:10.1016/0168-9002(94)01526-0`

[7] L. Liu *et al.*, "Sirius Commissioning Results and Operation Status", in *Proc. IPAC'21*, Campinas, Brazil, May 2021, pp. 13-18. `doi:10.18429/JACoW-IPAC2021-MOXA03`

[8] O Laboratório Nacional de Luz Síncrotron – LNLS, `https://www.lnls.cnpem.br/sobre/`, accessed on 16 October 2023.

[9] Final Report of the NASA Technology Readiness Assessment (TRA) Study Team, `https://ntrs.nasa.gov/api/citations/20170005794/downloads/20170005794.pdf`, accessed on 16 October 2023.

[10] S. Takeda, “Development of New Hydrostatic Levelling Equipment for Large Next Generation Accelerator”, in *Proc. EPAC'04*, Lucerne, Switzerland, Jul. 2004, paper WEPLT113, pp. 2113-2115.

[11] S. R. Marques *et al.*, “Improvements on Sirius Beam Stability”, in *Proc. IPAC'22*, Bangkok, Thailand, Jun. 2022, pp. 226-229. `doi:10.18429/JACoW-IPAC2022-MOPOPT002`

[12] D. Blitzkow *et al.*, “First Results Using the Microg LaCoste for Developping an Earth Tide Model in São Paulo”, in *Proc. Thirteenth International Congress of the Brazilian Geophysical Society*, Rio de Janeiro, Brazil, Aug. 2013. `doi:10.1190/sbgf2013-372`

[13] T. Hartmann and H. Wenzel. “The HW95 tidal potential catalogue”, *Geophys. Res. Lett.*, p. 22-24, Dec. 1995. doi:10.1029/95GL03324

[14] S. R. Marques *et al.*, “Improvements on Sirius Beam Stability”, in *Proc. IPAC'22*, Bangkok, Thailand, Jun. 2022, pp. 226-229. `doi:10.18429/JACoW-IPAC2022-MOPOPT002`